Biophysical Journal
Article

Biophysical Society

Synaptobrevin-2 C-Terminal Flexible Region Regulates the Discharge of Catecholamine Molecules

Annita N. Weiss[1,*]
[1]Laboratory for Nanoscale Cell Biology, Max-Planck-Institute for Biophysical Chemistry, Göttingen, Germany

ABSTRACT The discharge of neurotransmitters from vesicles is a regulated process. Synaptobrevin-2, a snap receptor (SNARE) protein, participates in this process by interacting with other SNARE and associated proteins. Synaptobrevin-2 transmembrane domain is embedded into the vesicle lipid bilayer except for its last three residues. These residues are hydrophilic and constitute synaptobrevin-2 C-terminal flexible region. The residue Y113 of synaptobrevin-2 flexible region was mutated to lysine and glutamate. The effects of these mutations on the exocytotic process in chromaffin cells were assessed using capacitance measurements combined with amperometry and stimulation by flash photolysis of caged Ca^{2+}. Both Y113E and Y113K mutations reduced the number of fusion-competent vesicles and reduced the rates of release of catecholamine molecules in quanta release events. These results exclude any direct interaction of this domain with the catecholamine molecules that are escaping through the fusion pore but favor its interaction with the vesicle membrane as a mean of regulating exocytosis.

INTRODUCTION

A series of successful events are required for the discharge of vesicular contents. These events include a priming step, during which vesicles that are docked at the cell plasma membrane wait for the local influx of calcium to quickly fuse with the cell plasma membrane (1,2). This priming step is followed by the formation of the fusion pore and the discharge of the vesicular content (3–5). Synaptobrevin-2/Vamp-2 (SybII), a snap receptor (SNARE) protein, participates in these events through the interaction of its domains with the vesicle lipid bilayer (6) and with other SNARE proteins, namely syntaxin and the synaptosome-associated protein of 25 kilodalton (SNAP-25) (7,8). SybII N-terminal domain mutations that disrupt the interactions between SybII and its SNARE partners lead to a reduction in the number of fusion-competent vesicles, whereas its C-terminal domain mutations reduce the speed at which vesicles discharge their contents (9,10). Furthermore, SybII interaction with the vesicle lipid bilayer is established through its transmembrane domain. This domain is composed mostly of hydrophobic residues. The deletion (11), replacement by artificial lipid anchors (12–14), or extension by polar residues (6) of the SybII transmembrane domain partially to completely obstructs the fusion process. The details of SybII transmembrane domain interactions with syntaxin have been revealed by the crystal structure of the SNARE complex that includes the transmembrane domains of these two proteins. The crystal structure shows that the last residues of SybII and syntaxin transmembrane domains do not form hydrogen bonds. This lack of interactions leaves SybII C-terminal domain residues freely available to interact with the vesicle lipid phosphate headgroups (15). This region of SybII constitutes its flexible region. The relevance of this flexible region during the discharge of catecholamine in chromaffin cells is investigated.

MATERIALS AND METHODS

Single cell expression

Single chromaffin cells were isolated by an enzymatic reaction from medulla glands of E17 to E19 embryonic littermate. These double knockout (DKO) cells lacked both SybII and cellubrevin. The complementary DNAs encoding for SybII-Y113E and SybII-Y113K were produced by polymeric chain reaction and verified by complementary DNA sequencing. The cells were infected using the Semliki Forest Viral expression system, 3–4 days after culture (16).

Electrophysiology

Individual chromaffin cells were infected for 4 or 5 h to allow for the dual expression of enhanced green fluorescent protein and SybII. Flash photolysis and capacitance measurements were carried out at whole-cell patch

Submitted April 6, 2018, and accepted for publication January 24, 2019.
*Correspondence: angatch@gwdg.de
Editor: Heping Cheng.
https://doi.org/10.1016/j.bpj.2019.01.028

configuration by infusing 0.4 M fura-4F, 0.4 M mag-fura-2 (Molecular Probes, Eugene, OR), and 0.4 M $CaCl_2$ bound to 0.5 M nitrophenyl-EGTA. Ratiometric fluorescent measurements for the detection of calcium were performed as previously described (6).

Single-vesicle capacitance measurements were performed at cell-attached patch configuration. The bath solution contained the following: 145 mM NaCl, 1 mM $MgCl_2$, 2.8 mM KCl, 2 mM $CaCl_2$, and 10 mM HEPES, for which the pH and osmolarity were adjusted to 7.2 with NaOH and to 310 milliosmoles with D-glucose whenever necessary. The pipette solution contained 50 mM NaCl, 100 mM TEA-Cl, 5 mM KCl, 5 mM $CaCl_2$, 1 mM $MgCl_2$, and 10 mM HEPES/NaOH (pH 7.2). The experiments were performed using the EPC-7 amplifier (HEKA) and a lock-in amplifier (SR 830; Stanford Research Systems, Sunnyvale, CA). A 20 KHz, 50 mV sine wave stimulus at 100 mV/pA was used to resolve single capacitance steps. The phase was calibrated by applying the Neher-Marty method (17), which consists of applying a capacitance dithering to change the value of the capacitance while leaving the conductance intact. This was then used offline to adjust the phase such that no changes were observed only in the conductance trace. From the admittance of the cell-attached patch traces, single capacitance step sizes and conductance were calculated using IgorPro software (Wavemetrics, Lake Oswego, OR). The fusion pore conductance analysis was restricted to the detection of the initial conductance taken within 10% of the vesicle full fusion. Because the sizes of the capacitance steps were small and the fusion pore lifetimes were less than 15 ms, the subsequent fusion pore expansion values were likely skewed by the lock-in amplifier low-pass filter set to 1 ms, 24 dB (18,19). Thus, the fusion pore duration and conductance rates were not included in the analysis.

Amperometry

The high-resolution amperometry measurement was used to detect the secretion of catecholamine molecules from individual vesicles by using a conventional carbon fiber with a 10-μM diameter. To minimize errors due to diffusion, the carbon fiber was pressed onto the cell membrane and the tip of the electrode was freshly cut before each data acquisition. The oxidations of molecules at the surface of the electrode were detected as amperometry spikes. Amperometry currents were acquired using the EPC-7 amplifier at a sampling frequency of 20 kHz and filtered at 3 kHz. Cells were stimulated for secretion by infusing them at whole-cell configuration with a solution containing the following: 100 mM Cs-glutamate, 0.3 mM Na-GTP, 2 mM Mg-ATP, 2.5 mM $CaCl_2$, 0.4 mM fura-4F, 0.4 mM furaptra, 20 mM DPTA, and 32 mM HEPES (pH 7.2). The data are presented as means of medians, and one-way ANOVA was used for statistical analysis ($*p < 0.05$, $**p < 0.01$).

Immunofluorescence

To investigate SybII localization, SybII and chromogranin immunostaining were compared. DKO chromaffin cells were cultured in glass-bottom dishes (35/12 mm, glass thickness: 0.17 mm; Warner Instruments, Hamden, CT). Cells were fixed 4 h after viral infection with 3.7% formaldehyde for 20 min at room temperature. They were subsequently washed in phosphate-buffered saline (PBS), permeabilized for 10 min in 0.1% triton X-100, and neutralized with 50 mM NH_4Cl. They were then incubated for 2 h with monoclonal primary antibodies (mouse anti-SybII; Synaptic Systems, Göttingen, Germany) and chromogranin A antibody (Abcam, Cambridge, UK), both diluted at 1:500 in 10% bovine serum albumin. This was followed by a 10 min wash in PBS. Cells were then exposed to secondary antibodies cyanine (Cy)3-conjugated goat anti-mouse dilution 1:200 and cyanine (Cy)-5 conjugated rabbit anti-mouse dilution 1:200 for 1 h at room temperature. Then they were washed five times with PBS, incubated with secondary antibodies (1:200 dilutions; Invitrogen, Carlsbad, CA) for 1 h, washed, and mounted or kept in PBS overnight at 4°C. Fluorescent intensities of region of interest-containing cells were quantified. For display, alignments of the images were performed manually using ImageJ.

Membrane potential calculation

The change in membrane intravesicular potential was calculated given that, before the merger of the vesicle membrane with the plasma membrane, the potential differences across the vesicle membrane (V_v) and the cell plasma membrane (V_c) differ. However, when a connection between the two membranes is established, the vesicular membrane potential must reach the cell membrane potential resting state. The time dependence of this process is calculated according to

$$\Delta V_v(t) = V_c + V_{v0} - (1/C_v)\int_0^t I_p(t')dt' \qquad (1)$$

where $V_c = -70$ mV is the cell membrane potential, and $V_{v0} = +50$ mV is the intravesicular potential before fusion in the presence of ATP and Mg^{2+} (20). During the initiation of the fusion pore, at t = 0, the intravesicular potential is, therefore, $V(t = 0) = (V_c + V_{v0}) = +20$ mV. In addition, the vesicle capacitance change is also modified by SybII C-terminal residues according to the energy that is required to move these residues from water to the membrane-water interface G*wif* (6)

$$C_v = A\exp(Gwif) + B \qquad (2)$$

where A = 1 and B = 0. The time constant for charging the capacitor was assumed to be 10 μs. The change in the intravesicular potential is facilitated by the flow of ions through the fusion pore (21). The current through the fusion pore because of the exchange of ions is calculated according to the Nernst-Planck electrodiffusion equations using parameters as previously defined (22).

$$I_p = -D.\frac{a}{l}.z^2.\frac{\Delta V_v F^2}{RT}\,\frac{[S_v] - [S_e]\exp(-z\Delta V_v/RT)}{1 - \exp(-z\Delta V_v F/RT)} \qquad (3)$$

The concentration of catecholamine in a vesicle assumed here is S_v = 135 mM (22) and its external concentration is S_e = 0 mM.

RESULTS

The full-length SNARE complex is stabilized by many interactions, including the formation of hydrogen bonds between SybII and syntaxin. In addition, Van der Waals surface interactions also help to maintain this structure except for the last three residues of SybII, which are polar (Fig.1).

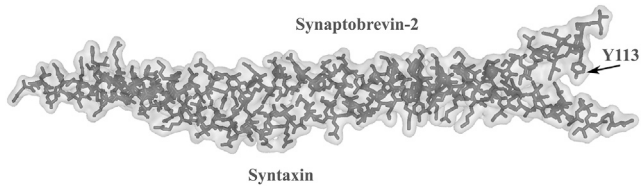

FIGURE 1 Van der Waals space-filling model of SybII and syntaxin full structure. The Van der Waals space-filling model was generated from the already published crystal structure (Protein Data Bank [PDB]: 3HD7 (15)). The hydrophilic flexible region of SybII transmembrane starts at residue Y113. This flexible region does not interact with syntaxin transmembrane domain after the SNARE complex is formed. Tyrosine residue at position 113 was mutated to single lysine (SybII-Y113K) or glutamate (SybII-Y113E).

These residues form the SybII transmembrane domain flexible region. To destabilize this flexible region, a single residue Y113 was mutated to lysine or glutamate. This location was chosen because prior investigation showed that charged amino acids at the end of SybII C-terminal completely inhibit vesicle fusion (6). The gain-of-functions of the mutated constructs were assessed after their expressions in null DKO chromaffin cells. The fusion of vesicles with the cell plasma membrane was triggered by infusing photo-releasable calcium into cells at whole-cell patch configuration. The exocytotic response was monitored by parallel detection of the cell membrane capacitance and the release of associated catecholamine by amperometry measurement.

Charged residues in SybII flexible region partially support vesicle fusion

SybII wild-type protein was expressed in DKO embryonic chromaffin cells. The exocytotic response to the rapid influx of intracellular calcium was a biphasic increase of the capacitance trace. The capacitance trace could be sectioned into two phases: a burst phase representing a rapid change of the capacitance amplitude and a sustained phase that lasted many seconds (Fig. 2 *A*). The two phases reflect vesicles that fuse with fast and slow kinetics. The burst and the sustained phases of cells expressing SybII-Y113K and SybII-Y113E were reduced by ~50% in comparison to the capacitance phases of cells expressing SybII (Fig. 2, *C* and *D*). Furthermore, when the capacitance traces were scaled to the same amplitudes at 0.5 s after the calcium stimulus,

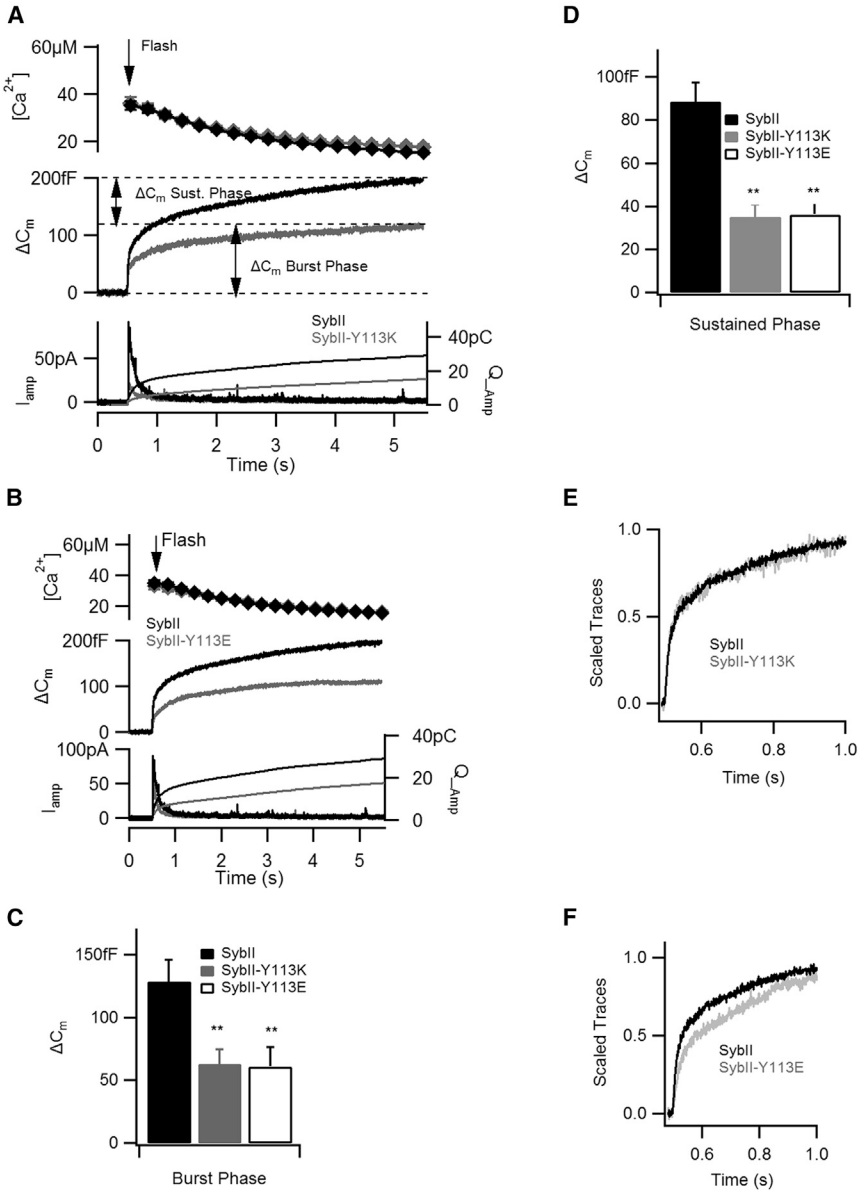

FIGURE 2 Charged residues within the transmembrane domain of SybII partially rescue the exocytosis phenotype at whole-cell patch. The fusion of vesicles was stimulated by releasing caged calcium in patched cells. (*A* and *B*) At comparable $[Ca^{2+}]_i$ increase (*top*), cells expressing SybII-Y113K (n = 20) and (*B*) SybII-Y113E (n = 22) showed a reduction of capacitance amplitudes (*middle*) and a reduction of amperometry currents (*bottom*) in comparison to SybII (n = 18)-overexpressing cells. The capacitance amplitudes were biphasic. The burst phase was calculated as the capacitance change at 0.5 s after the release of calcium (Flash). The sustained phase was calculated as the capacitance change between 0.5 and 5 s. (*C* and *D*) Cells expressing SybII-Y113K and SybII-Y113E had reduced burst and the sustained phases. (*E* and *F*) Only SybII-Y113E slowed the kinetic of the burst phase (**$p < 0.01$).

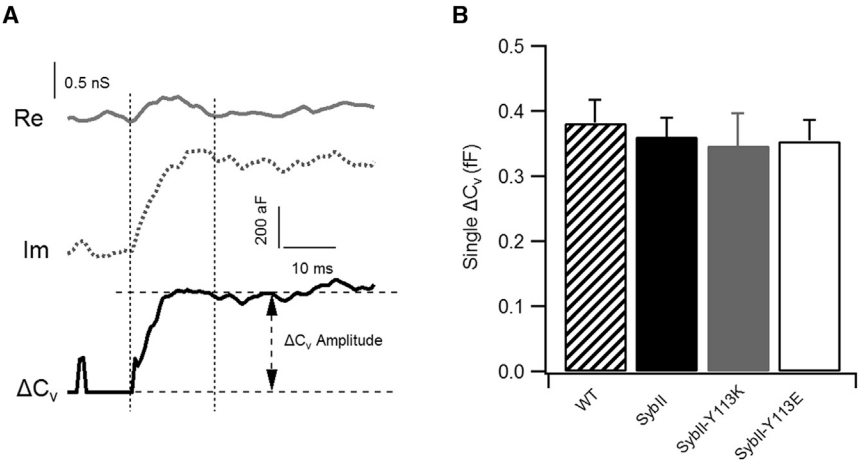

FIGURE 3 Single capacitance measurement by cell-attached capacitance. (*A*) The real part (Re, *gray line*) and the imaginary part (Im, *dashed line*) were calculated from the admittance measurement. The imaginary part and the real part provide information about the vesicle capacitance C_v. (*B*) Noninfected embryonic chromaffin cells (n = 21 cells, 173 events) and cell expressing SybII (n = 11 cells, 50 events), SybII-Y113K (n = 14 cells, 52 events), and SybII-Y113E (n = 11 cells, 79 events) all had similar vesicle capacitance step sizes.

only SybII-Y113E displayed a slower burst kinetic (Fig. 2, *E* and *F*). Altogether, these data suggest that both mutations inhibit the fusion of rapid and slow fusing vesicles.

Next, the fusion of individual vesicles of cells expressing SybII-Y113K and SybII-Y113E were probed to determine whether the above-observed phenotype could be explained by a reduction of their sizes. The fusion of a single vesicle with the cell plasma membrane causes a stepwise increase of the capacitance when it is probed at cell-attached patch-clamp configuration. The current that was detected during these measurements was analyzed to extract the impedance properties (21). The real part of the patch admittance and the increase in the imaginary part were used to calculate the vesicle capacitance change (C_v) (Fig. 3 *A*). The mean ± standard error of the mean capacitance step sizes of embryonic chromaffin cells overexpressing SybII (0.36 ± 0.02 fF) was similar to the average step size recorded in wild-type noninfected cells (0.38 ± 0.03 fF) (Fig. 3 *B*). Also, cells expressing SybII-Y113K (0.34 ± 0.04 fF) and SybII-Y113E (0.35 ± 0.03 fF) had comparable step sizes as SybII-expressing cells. The average vesicle size of ∼55 nm calculated from these capacitance measurements is consistent with mouse embryonic vesicle sizes previously determined (23–25). This result indicates the mutations did not alter the size of vesicles.

The fusion pore conductance can also be calculated from the time resolved of the patch admittance. The initial fusion pore conductance taken within 10% of the vesicle full fusion was similar for all constructs: noninfected cells (77.08 ± 0.04 pS), cells overexpressing SybII (70.08 ± 0.08 pS), SybII-Y113K (72.30 ± 0.12 pS), and SybII-Y113E (69.22 ± 0.08pS). The subsequent fusion pore expansion could not reliably be estimated because of the rapid expansion of the fusion pore (19,26).

Synapobrevin-2 C-terminus flexible region regulates the flux of catecholamine

An indirect way to assess the fusion pore conductance is to monitor the flux of catecholamine during its discharge through the fusion pore. Therefore, the release of catecholamine from individual vesicles was monitored after the infusion of cells with calcium. Catecholamine molecules were expulsed from vesicles oxidized at the surface of a potentiated carbon fiber electrode that was pressed onto the cell membrane. The resulting amperometric current spikes were analyzed to extract the fusion pore characteristics (Fig. 4 *A*). The total amount of catecholamine molecules released from individual vesicles was similar for cells that expressed SybII or the mutated proteins (Fig. 4 *B*). This is consistent with the above result, which shows that these cells had similar vesicle sizes (Fig. 3 *B*) and also indicates that the mutated SybII did not modify the catecholamine content of vesicles. The mean current amplitude of SybII-Y113E had the lowest peak amplitude (22 ± 2 pA) followed by SybII-Y113K (36 ± 4 pA); this is in comparison to 56 ± 6 pA for SybII (Fig. 4 *C*), indicating a slower diffusion of catecholamine molecules through the fusion pore. This is also consistent with a broader spike half-width observed in SybII-Y113E (Fig. 4 *D*). The amperometry spike is often preceded by a "foot" that reflects the formation of a metastable fusion pore, which allows for an initial leakage of molecules. The mean foot duration was longer for SybII-Y113E (7.3 ± 0.4 ms) and SybII-Y113K (5.5 ± 0.5 ms) in comparison to SybII (5.0 ± 0.3 ms), albeit only the foot duration of SybII-Y113E was significantly longer (Fig. 4 *E*). The foot amplitudes and the foot quanta release, on the other hand, were significantly smaller (Fig. 4, *F* and *G*) for both mutations, indicating that only few catecholamine molecules could diffuse through the initial fusion pore.

To assess whether SybII mutations modified the fusion pore structure, the occurrence of events displaying a foot was quantified. SybII mutations reduced the number of detectable events/min. 23 events/min were measured in SybII-expressing cells in comparison to 17 events/min and 15 events/min for SybII-Y113E and SybII-Y113K, respectively. Some of the detectable amperometry events displayed a "foot." The occurrence of these events was the same for all constructs (Fig. 5). Occasionally, events that

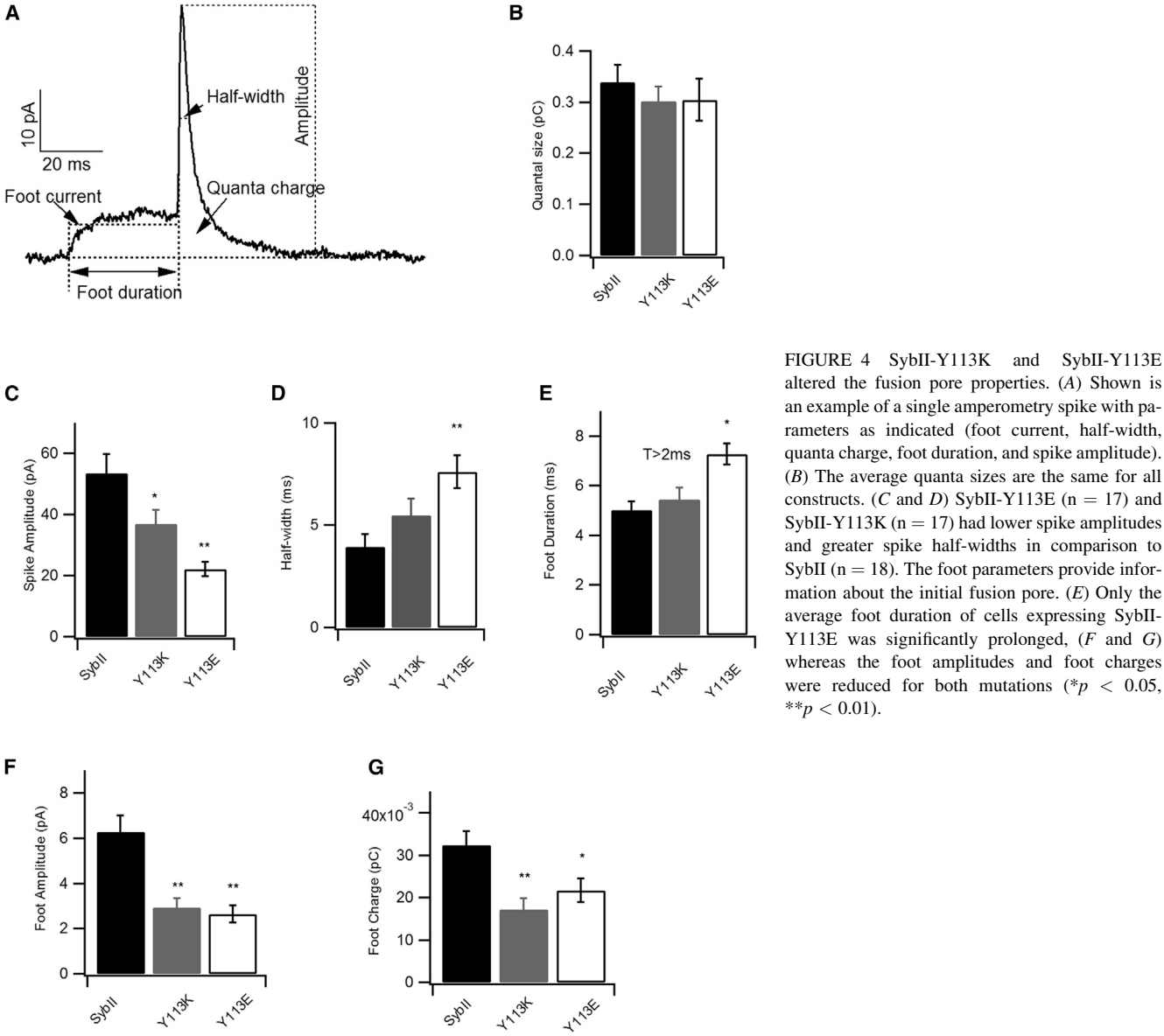

FIGURE 4 SybII-Y113K and SybII-Y113E altered the fusion pore properties. (*A*) Shown is an example of a single amperometry spike with parameters as indicated (foot current, half-width, quanta charge, foot duration, and spike amplitude). (*B*) The average quanta sizes are the same for all constructs. (*C* and *D*) SybII-Y113E (n = 17) and SybII-Y113K (n = 17) had lower spike amplitudes and greater spike half-widths in comparison to SybII (n = 18). The foot parameters provide information about the initial fusion pore. (*E*) Only the average foot duration of cells expressing SybII-Y113E was significantly prolonged, (*F* and *G*) whereas the foot amplitudes and foot charges were reduced for both mutations (*$p < 0.05$, **$p < 0.01$).

never fully dilated were observed. These events have been coined "stand-alone" events (27) and are characterized by a rapid rise and rapid fluctuations with an amplitude characteristic of a foot signal (Fig. 5 *B*). Only ~4 and ~3% of SybII-Y113K and SybII-113E events were stand-alone in comparison to ~8% of SybII events (Fig. 5 *C*), suggesting that this subpopulation of amperometry events, which displayed a restriction of fusion pore dilation, was also inhibited by the mutations.

To demonstrate the vesicular localization of SybII constructs, cells were fixed and immunolabeled with chromogranin and SybII antibodies. Although SybII showed fluorescent puncta in nontransfected cells (Fig. 6 *A*), the viral expression of SybII constructs produced diffuse SybII fluorescence because the virus induced SybII expression in granular compartments as well as on the cell plasma membrane. This is typical for viral expression of proteins (9). Nevertheless, SybII fluorescence occasionally colocalized with chromogranin fluorescence, which showed granular structures (Fig. 6, *A–C*). This indicates that the mutations did not prevent the vesicular localization of SybII. The overexpression of SybII was also quantified. The genetic depletion of SybII resulted in ~70% less of the protein expression (Fig. 6 *E*). At this range, the complete inhibition of the fusion of vesicles is expected (23). Its overexpression as well as the overexpression of the mutants led to three to fourfold more proteins above the endogenous level (wild-type).

DISCUSSION

The C-terminal end of the SybII transmembrane region consists of hydrophilic residues. Unlike other domains of SybII,

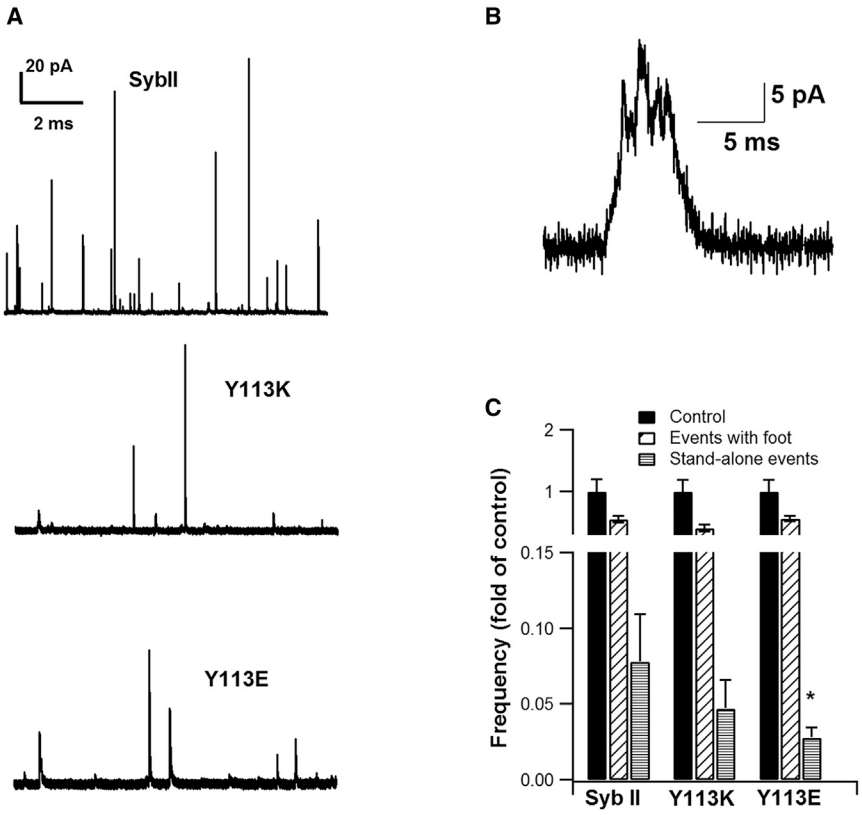

FIGURE 5 Fraction of stand-alone and amperometry events with a preceding foot. (*A*) Examples of SybII amperometry traces recorded from cells expressing SybII (*left*), SybII-Y113K (*middle*), and SybII-Y113E (*right*) are shown. SybII mutations reduced the number of detectable events/min. 23 events/min was measured in SybII-expressing cells in comparison to 17 events/min and 15 events/min for SybII-Y113E and SybII-Y113K, respectively. (*B*) An example of an amperometry stand-alone event is shown. (*C*) The fraction of amperometry events with preceding foot and fraction of stand-alone events were compared to the normalized total number of spikes (control) for each construct. The SybII-Y113E mutation reduced the fraction of stand-alone events ($*p < 0.05$).

this region does not interact with syntaxin after the formation of the SNARE complex (15). This is likely to facilitate the interaction of the SybII C-terminal region with the vesicle membrane lipid headgroups and to facilitate the initiation of the fusion pore (6). In this study, the tyrosine residue at position 113 of the SybII transmembrane region was substituted with charged amino acids lysine and glutamate. Although these mutations still support the fusion of vesicles, these were to a lesser extent than the wild-type SybII protein, as evidenced by a partial reduction of the burst and the sustained phases of the capacitance amplitudes, the reduction of the amperometry spike frequencies, and the lower occurrence of stand-alone events. Given the location of these mutations within the SybII flexible domain, they likely did not interfere with the zippering of the SNARE complex (15) because the SNARE complex formation proceeds from the N- to the C-terminus (28). However, the substituting lysine or glutamate residues may have altered the flexibility of this SybII domain by stabilizing it to the vesicle lipid bilayer through electrostatic interactions. A rigid SybII transmembrane domain causes fewer vesicles to fuse and also induces a slower expansion of the fusion pore (29).

Although the lysine and glutamate residues are, respectively, positively and negatively charged, both SybII-Y113K and SybII-Y113E showed a reduction of the foot amplitude and foot charge, suggesting that the mutations did not interfere with the flux of catecholamine through the fusion pore, therefore excluding a direct electrostatic effect of these residues on the catecholamine flux. Furthermore, the possibility that the side chains of the lysine and glutamate residues could have induced a steric occlusion of the fusion pore, rendering the fusion pore smaller and reducing the flux of catecholamine molecules, was also excluded. First, tyrosine has a side chain volume (193.6 A^3) greater than the substituted residue volumes (lysine, 168.6 A^3 and glutamate, 138.4 A^3) (30). Second, Y113 has also previously been mutated to tryptophan (227.8 A^3), which has a side chain volume that is greater; nevertheless, the flux of catecholamine through the fusion pore slightly increased (24). However, the reduction of catecholamine flux through the fusion pore directly correlated with the nature of the substituted amino acids, that is, their energies of transfer ($\Delta Gwif$) from water to the water-membrane interface (Fig.7 *A*). The lysine and the glutamate mutations may have also altered the intravesicular potential, thereby reducing the flux of ions through the fusion pore, hence the secretion of catecholamine. This would have occurred during the first milliseconds of the fusion pore formation.

SybII C-terminal flexible region can modify the intravesicular potential

The amperometry measurement of the discharge of catecholamine from single vesicles suggests that the fusion of a vesicle starts with the formation of the fusion pore followed by its expansion. Yet, what is often overlooked is the fact that

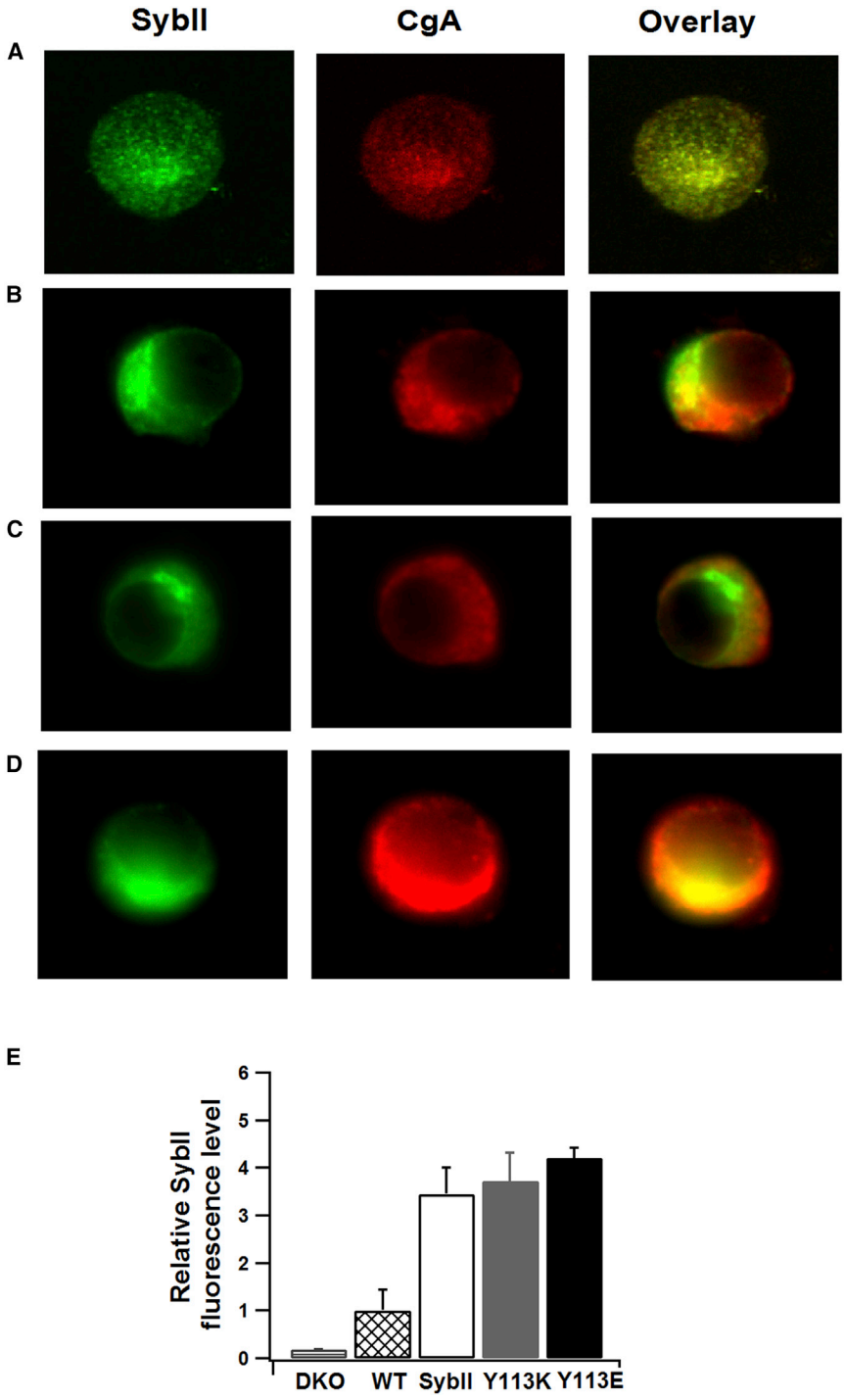

FIGURE 6 SybII overexpression and colocalization. SybII isoforms in embryonic mouse chromaffin cells are shown. (*A*) Exemplary images of wild-type (WT) noninfected cell, (*B*) SybII overexpression, (*C*) SybII-Y113K, and (*D*) SybII-Y113E are shown. The immunolabeling of chromogranin (anti-CgA, *red*) in fixed mouse embryonal chromaffin cells showed granulated features. SybII staining (*green*) fluorescence is spread. The overlay of the images shows overlapped areas. (*E*) SybII, SybII-Y113K, and SybII-Y113E were overexpressed three- to fourfold above wild-type level. SybII (n = 22), SybII-Y113E (n = 27), SybII-Y113K (n = 20), and double knockout (DKO, n = 39) fluorescence were normalized to WT noninfected cells (n = 21). To see this figure in color, go online.

during this process, the vesicle membrane whose potential is initially distinct from that of the cell membrane potential must reach the resting cell membrane potential (21) during the first milliseconds of fusion pore opening. Tyrosine's preferred location is the vesicle lipid bilayer region that contains water and the lipid polar headgroups (31,32). At this position, the mutations would alter the intravesicular potential when incorporated into the membrane-water interface during the fusion pore formation (6).

The effects of lysine and glutamate side chains on the intravesicular potential during the fusion pore opening was assessed by calculating the intravesicular potential given that the capacitance change resulting from the vesicle fusion with the cell plasma membrane depends exponentially on the free energy of transfer (ΔG_{wif}) of SybII C-terminal residues from water to the water-membrane interface (6). The free energy of transfer (ΔG_{wif}) for tyrosine was used as the reference in these calculations. At the

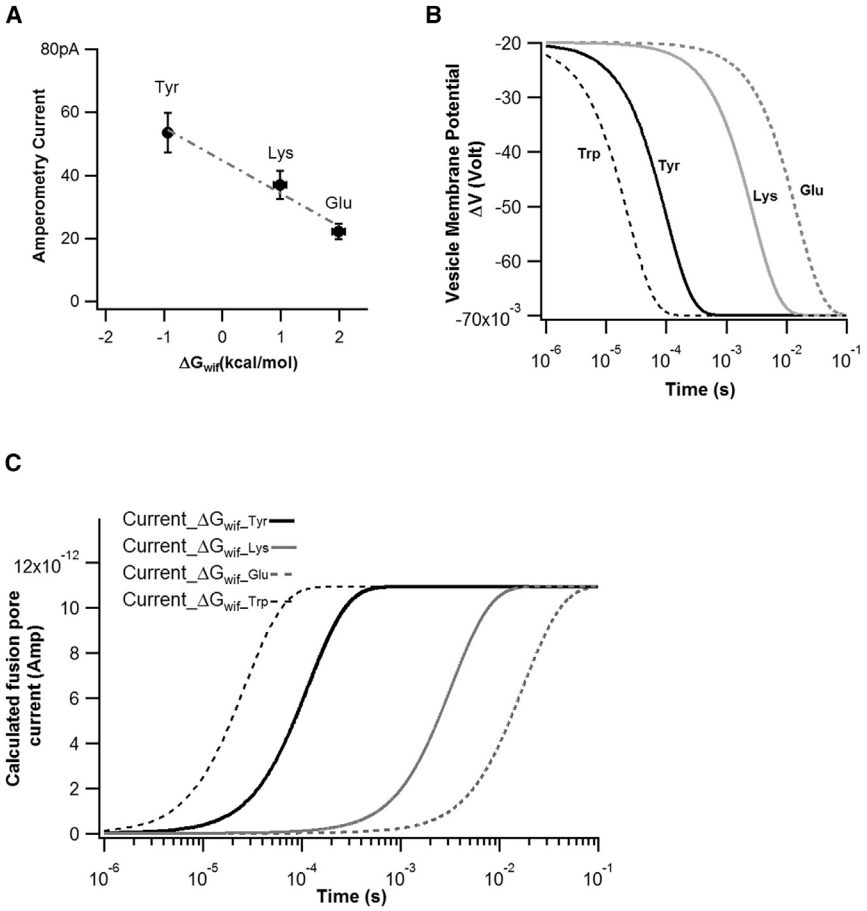

FIGURE 7 SybII transmembrane domain mutations, SybII-Y113K and SybII-Y113E, modify the intravesicular potential. (*A*) The currents were experimentally determined (Fig.4 *C*). They are the average spike amplitude for SybII, SybII-Y113K, and SybII-Y113E. They are plotted against the energy that is required to transfer tyrosine, lysine, or glutamate residues from water into the lipid bilayer interface (33). (*B* and *C*) The current and the change in intravesicular membrane potential are evaluated for the residues tyrosine, glutamate, lysine, and tryptophan while taking into consideration the free energy of transfer of these residues from water into the water-lipid bilayer interface. Tryptophan was added for comparison because Y113 was previously mutated to tryptophan (24). These analyses indicate that when the fusion pore opens, the intravesicular potential begins to change while the current flows through the fusion pore. The intravesicular potential equilibrium is slowed when the energy of transfer (ΔG_{wif}) of the mutated residues is higher.

onset of the fusion of a vesicle, the intravesicular potential is 50 mV (20). During the fusion pore expansion, the intravesicular potential needs to equilibrate to the membrane potential (−70 mV). However, the energies of transfer ($\Delta Gwif$) for lysine and glutamate are higher than the energy of tyrosine (33); correspondingly, the intravesicular potentials would take longer to equilibrate to the cell membrane potential (Fig. 7 *B*). This is due to side chains of the lysine and glutamate residues that are incorporated into the vesicle membrane.

The intravesicular equipotential is facilitated by the flux of ions through the fusion pore (21,34). This flux was calculated using the Nernst-Planck equation. The current flowing through the fusion pore was smaller when the energy $\Delta Gwif$ of lysine or glutamate was considered. These currents were compared to the calculated current obtained considering the energy ($\Delta Gwif$) of tyrosine (Fig. 7, *B* and *C*). Also, in a recent study, Y113 was mutated to tryptophan (24). Tryptophan is similar to tyrosine as it is found mainly at the water-lipid bilayer interface (32). Tryptophan in the membrane would speed the intravesicular potential equilibrium (Fig. 7), thus speeding the flux of catecholamine, as previously observed (24). This analysis therefore suggests that SybII mutations, SybII-Y113K and SybII-Y113E, likely slowed the intravesicular potential equilibrium rate, thereby also slowing the initial flux of catecholamine molecules. This analysis is consistent with previous findings that show that increasing the membrane potential of bovine chromaffin cells (35) or reducing the extracellular concentration of sodium ions alters the catecholamine flux through the fusion pore (22,36). Therefore, similarly to catecholamine influx into the vesicle (20), its efflux may also be coupled to the intravesicular potential.

CONCLUSION

This work provides an insight into how the flexible transmembrane domain of SybII can modulate the release of catecholamine during its escape through the fusion pore. It suggests that this modulation is achieved through the interaction of the SybII flexible region with the vesicle membrane rather than through a direct interaction with the catecholamine molecules.

AUTHOR CONTRIBUTIONS

A.N.W designed and performed the flash photolysis of caged calcium to measure capacitance membranes, the single vesicle capacitance measurements, and the amperometry measurements and acquired the immunofluorescence data. A.N.W. also performed all related analysis and wrote the manuscript.

ACKNOWLEDGMENTS

The author thanks Dirk Reuter and Ina Herfort for their expert technical assistance and to Dr. Manfred Lindau and Dr. Jakob Sørensen for their critical reading of the manuscript.

This work was supported by the National Institutes of Health grants R01NS38200, R01GM085808, and T32GM007469, and the Nanobiotechnology Center (a National Science Foundation Science and Technology Center, agreement ECS-9876771).

REFERENCES

1. Jahn, R., and D. Fasshauer. 2012. Molecular machines governing exocytosis of synaptic vesicles. *Nature.* 490:201–207.
2. Sørensen, J. B. 2009. Conflicting views on the membrane fusion machinery and the fusion pore. *Annu. Rev. Cell Dev. Biol.* 25:513–537.
3. Chen, Y. A., and R. H. Scheller. 2001. SNARE-mediated membrane fusion. *Nat. Rev. Mol. Cell Biol.* 2:98–106.
4. Fang, Q., and M. Lindau. 2014. How could SNARE proteins open a fusion pore? *Physiology (Bethesda).* 29:278–285.
5. Sørensen, J. B. 2005. SNARE complexes prepare for membrane fusion. *Trends Neurosci.* 28:453–455.
6. Ngatchou, A. N., K. Kisler, …, M. Lindau. 2010. Role of the synaptobrevin C terminus in fusion pore formation. *Proc. Natl. Acad. Sci. USA.* 107:18463–18468.
7. Hanson, P. I., R. Roth, …, J. E. Heuser. 1997. Structure and conformational changes in NSF and its membrane receptor complexes visualized by quick-freeze/deep-etch electron microscopy. *Cell.* 90:523–535.
8. Söllner, T., S. W. Whiteheart, …, J. E. Rothman. 1993. SNAP receptors implicated in vesicle targeting and fusion. *Nature.* 362:318–324.
9. Walter, A. M., K. Wiederhold, …, J. B. Sørensen. 2010. Synaptobrevin N-terminally bound to syntaxin-SNAP-25 defines the primed vesicle state in regulated exocytosis. *J. Cell Biol.* 188:401–413.
10. Martens, S., and H. T. McMahon. 2008. Mechanisms of membrane fusion: disparate players and common principles. *Nat. Rev. Mol. Cell Biol.* 9:543–556.
11. Fdez, E., M. Martínez-Salvador, …, S. Hilfiker. 2010. Transmembrane-domain determinants for SNARE-mediated membrane fusion. *J. Cell Sci.* 123:2473–2480.
12. Chang, C. W., C. W. Chiang, …, M. B. Jackson. 2016. Lipid-anchored synaptobrevin provides little or no support for exocytosis or liposome fusion. *J. Biol. Chem.* 291:2848–2857.
13. McNew, J. A., T. Weber, …, J. E. Rothman. 2000. Close is not enough: SNARE-dependent membrane fusion requires an active mechanism that transduces force to membrane anchors. *J. Cell Biol.* 150:105–117.
14. Pieren, M., Y. Desfougères, …, A. Mayer. 2015. Vacuolar SNARE protein transmembrane domains serve as nonspecific membrane anchors with unequal roles in lipid mixing. *J. Biol. Chem.* 290:12821–12832.
15. Stein, A., G. Weber, …, R. Jahn. 2009. Helical extension of the neuronal SNARE complex into the membrane. *Nature.* 460:525–528.
16. Ashery, U., A. Betz, …, J. Rettig. 1999. An efficient method for infection of adrenal chromaffin cells using the Semliki Forest virus gene expression system. *Eur. J. Cell Biol.* 78:525–532.
17. Neher, E., and A. Marty. 1982. Discrete changes of cell membrane capacitance observed under conditions of enhanced secretion in bovine adrenal chromaffin cells. *Proc. Natl. Acad. Sci. USA.* 79:6712–6716.
18. Dernick, G., G. Alvarez de Toledo, and M. Lindau. 2003. Exocytosis of single chromaffin granules in cell-free inside-out membrane patches. *Nat. Cell Biol.* 5:358–362.
19. Fang, Q., K. Berberian, …, M. Lindau. 2008. The role of the C terminus of the SNARE protein SNAP-25 in fusion pore opening and a model for fusion pore mechanics. *Proc. Natl. Acad. Sci. USA.* 105:15388–15392.
20. Holz, R. W. 1979. Measurement of membrane potential of chromaffin granules by the accumulation of triphenylmethylphosphonium cation. *J. Biol. Chem.* 254:6703–6709.
21. Breckenridge, L. J., and W. Almers. 1987. Currents through the fusion pore that forms during exocytosis of a secretory vesicle. *Nature.* 328:814–817.
22. Gong, L. W., G. A. de Toledo, and M. Lindau. 2007. Exocytotic catecholamine release is not associated with cation flux through channels in the vesicle membrane but Na+ influx through the fusion pore. *Nat. Cell Biol.* 9:915–922.
23. Borisovska, M., Y. Zhao, …, D. Bruns. 2005. v-SNAREs control exocytosis of vesicles from priming to fusion. *EMBO J.* 24:2114–2126.
24. Chang, C. W., E. Hui, …, M. B. Jackson. 2015. A structural role for the synaptobrevin 2 transmembrane domain in dense-core vesicle fusion pores. *J. Neurosci.* 35:5772–5780.
25. Fang, Q., Y. Zhao, and M. Lindau. 2013. Juxtamembrane tryptophans of synaptobrevin 2 control the process of membrane fusion. *FEBS Lett.* 587:67–72.
26. Curran, M. J., F. S. Cohen, …, J. Zimmerberg. 1993. Exocytotic fusion pores exhibit semi-stable states. *J. Membr. Biol.* 133:61–75.
27. Zhou, Z., S. Misler, and R. H. Chow. 1996. Rapid fluctuations in transmitter release from single vesicles in bovine adrenal chromaffin cells. *Biophys. J.* 70:1543–1552.
28. Sørensen, J. B., K. Wiederhold, …, D. Fasshauer. 2006. Sequential N- to C-terminal SNARE complex assembly drives priming and fusion of secretory vesicles. *EMBO J.* 25:955–966.
29. Dhara, M., A. Yarzagaray, …, D. Bruns. 2016. v-SNARE transmembrane domains function as catalysts for vesicle fusion. *Elife.* 5:e17571.
30. Zamyatnin, A. A. 1972. Protein volume in solution. *Prog. Biophys. Mol. Biol.* 24:107–123.
31. MacCallum, J. L., W. F. Bennett, and D. P. Tieleman. 2008. Distribution of amino acids in a lipid bilayer from computer simulations. *Biophys. J.* 94:3393–3404.
32. Yau, W. M., W. C. Wimley, …, S. H. White. 1998. The preference of tryptophan for membrane interfaces. *Biochemistry.* 37:14713–14718.
33. Wimley, W. C., and S. H. White. 1996. Experimentally determined hydrophobicity scale for proteins at membrane interfaces. *Nat. Struct. Biol.* 3:842–848.
34. Lindau, M., and G. Alvarez de Toledo. 2003. The fusion pore. *Biochim. Biophys. Acta.* 1641:167–173.
35. Friedman, J. E., P. I. Lelkes, …, A. S. Schneider. 1985. Membrane potential and catecholamine secretion by bovine adrenal chromaffin cells: use of tetraphenylphosphonium distribution and carbocyanine dye fluorescence. *J. Neurochem.* 44:1391–1402.
36. Uvnas, B., and C.-H. Aborg. 1989. Role of ion exchange in release of biogenic amines. *Physiology (Bethesda).* 4:68–71.